

This article was downloaded by:

On: 25 January 2011

Access details: *Access Details: Free Access*

Publisher *Taylor & Francis*

Informa Ltd Registered in England and Wales Registered Number: 1072954 Registered office: Mortimer House, 37-41 Mortimer Street, London W1T 3JH, UK



## Liquid Crystals

Publication details, including instructions for authors and subscription information:

<http://www.informaworld.com/smpp/title~content=t713926090>

### On some liquid crystals made of banana-shaped molecules and their mixtures with rod-like molecules

N. V. Madhusudana<sup>a</sup>

<sup>a</sup> Raman Research Institute, Bangalore, India

First published on: 03 August 2009

**To cite this Article** Madhusudana, N. V.(2009) 'On some liquid crystals made of banana-shaped molecules and their mixtures with rod-like molecules', *Liquid Crystals*, 36: 10, 1173 – 1184, First published on: 03 August 2009 (iFirst)

**To link to this Article:** DOI: 10.1080/02678290903034100

**URL:** <http://dx.doi.org/10.1080/02678290903034100>

PLEASE SCROLL DOWN FOR ARTICLE

Full terms and conditions of use: <http://www.informaworld.com/terms-and-conditions-of-access.pdf>

This article may be used for research, teaching and private study purposes. Any substantial or systematic reproduction, re-distribution, re-selling, loan or sub-licensing, systematic supply or distribution in any form to anyone is expressly forbidden.

The publisher does not give any warranty express or implied or make any representation that the contents will be complete or accurate or up to date. The accuracy of any instructions, formulae and drug doses should be independently verified with primary sources. The publisher shall not be liable for any loss, actions, claims, proceedings, demand or costs or damages whatsoever or howsoever caused arising directly or indirectly in connection with or arising out of the use of this material.

## INVITED ARTICLE

### On some liquid crystals made of banana-shaped molecules and their mixtures with rod-like molecules

N.V. Madhusudana\*

Raman Research Institute, C.V. Raman Avenue, Bangalore 560 080, India.

(Received 15 April 2009; final form 10 May 2009)

Soft matter results from relatively weak interparticle interactions. Liquid crystals exhibit the largest variety of soft matter, and have fascinating physical properties and technological applications. de Gennes showed that the seemingly complex properties are often amenable to phenomenological descriptions, based on the underlying macroscopic symmetry of the medium. The latter ultimately depends on subtle intermolecular interactions, as exemplified by the discoveries of new types of liquid crystals made of banana-shaped (or bent-core (BC)) molecules. In this article, we review some aspects of these liquid crystals, with an emphasis on our own contributions. These include a simplified theoretical description of the most frequently observed  $B_6$ – $B_1$ – $B_2$  sequence of phases in homologous series of compounds with BC molecules, experimental studies on induced phases in mixtures of compounds with BC and rod-like molecules and on some novel properties exhibited in the nematic phase of such mixtures.

**Keywords:** bent-core molecules; mixtures of bent-core and rod-like molecules; induced phases

#### 1. Introduction

In his Nobel lecture de Gennes defined ‘soft matter’ as forms of matter that combine flexibility with complexity (1). Both of these properties ultimately arise because of relatively weak interparticle interactions. Of the various types of soft matter, liquid crystals exhibit the largest number of different types of organisations, which are characterised by different symmetries. The reason for this variety is that they combine the orientational order of anisotropically shaped molecules and spatial periodicity, usually in one or two dimensions (2, 3). Compounds with rod-shaped molecules are the most widely studied, and exhibit basically two types of liquid crystalline phases, namely, nematics with a pure orientational order and smectics with additional one-dimensional periodicity. If the molecules are chiral, many new structures and properties emerge (4). If the compounds are disc shaped, columnar liquid crystals with a two-dimensional periodicity result. The nematic phase is mainly stabilised for entropic reasons, although the Maier–Saupe mean field theory, which is based on anisotropic attractive intermolecular interactions, captures most of the essential features of the nematic-to-isotropic transition (2, 3). In most of the compounds studied, the smectic phase is exhibited by higher members of a homologous series. McMillan developed a molecular model of the layering order in the smectic A (SmA) phase by assuming a nano-segregation of the aliphatic and aromatic parts, which is

favoured by the internal energy of the medium, arising from dispersion interactions between the molecules (5). A similar argument is applicable for stabilising the columnar phase when the molecules are disc-like (6, 7). If the molecules are chiral, the director would like to have a spontaneous twist deformation. This can occur along two independent directions orthogonal to the director, and the resulting geometrical frustration leads to the blue phases close to the transition to the isotropic phase. The incompatibility between the layering order of smectics and a twist deformation in the layer plane leads to the formation of Abrikosov lattices in type II materials, (8, 9), which are arranged in the form of twist grain boundaries (10). In materials with extreme type II character, a three-dimensional modulation of the structure is found (11, 12).

Most of the compounds forming liquid crystals are polar in nature, but weak molecular dipoles do not have any notable influence on the structures. Strong longitudinal dipoles in rod-like molecules are very useful in lowering the operating voltages of various types of liquid crystal displays. In such materials, the dipolar contribution to the intermolecular energy can become comparable to the thermal energy, and the former favours an antiparallel orientation between neighbouring molecules (13). This means that even though the molecules are highly polar, the director retains its apolar character. The strongly polar cyano or nitro group is attached at one end of the aromatic

\*Email: nvmadhu@rri.res.in

core, and the aliphatic chain is attached at the other end. This leads to the generation of a new length, which is longer than the molecular length (14). Many compounds with such highly polar molecules exhibit unusual phenomena such as reentrant nematic and smectic phases and polymorphism of the smectic A phase (2).

The Landau theory of phase transitions is phenomenological in nature, and the only relevant physical input needed to describe a transition is the change in the symmetry between the two phases. One of the seminal contributions of de Gennes was to bring all of the phase transitions in liquid crystals known in the early 1970s under the fold of the Landau theory. In particular, by using the Landau theory he pointed out that the first-order nature of the nematic–isotropic transition arises from the second rank tensor order of the nematic, and that there is a close analogy between the smectic–nematic and superconductor–normal metal transitions (15). The unusual phenomena exhibited by compounds with highly polar molecules were in turn described by Prost (2) using two coupled smectic order parameters corresponding to the two lengths mentioned earlier.

## 2. Liquid crystals made of compounds with bent-core molecules

Bent-core (BC) or banana-shaped molecules are constructed by attaching aliphatic chains to the two ends of a bent aromatic core. Although they were first synthesised by Vorlander and Apel in the 1930s (16), the liquid crystalline phases exhibited by the compounds were not characterised (17). Similar compounds were made more recently by Matsunaga and Miyamoto (18), and subsequently their liquid crystalline phases were investigated (19). The BC molecules have shape polarity and deviate strongly from cylindrical symmetry (Figure 1).

Although many compounds with BC molecules are now known to form the uniaxial nematic phase, it is clear that polar packing of the BC molecules can lead to a layering order in which the molecules cannot rotate about their long (or bow) axes. The molecules

usually have moderate to large transverse dipole moments, and the polar packing results in polarised layers. If the molecules have a modest or zero tilt angle, the molecules can more easily fluctuate from one layer to a neighbouring layer if the two layers have antiferroelectric (AF) order (20). The AF structure is thus stabilised entropically, and is most frequently observed in compounds with BC molecules (21). On the other hand, attractive interactions between the end groups of molecules of neighbouring layers favour anticlinic correlations between the end groups, which can result in ferroelectric order at low temperatures (20). There can be intervening ferroelectric phases, in which the angle between the polarisation vectors of neighbouring layers can have a temperature-dependent azimuthal angle between  $0^\circ$  and  $180^\circ$ . The phenomenological axial next-nearest-neighbour  $xy$  model which predicts this sequence is similar to its chiral version which leads to exactly the opposite sequence found in smectic  $C^*$  liquid crystals made of chiral rod-like molecules (22, 23). The opposite sequences are simply a consequence of the very different geometrical shapes of the two types of molecules. There are just a few examples of the predicted sequence in compounds with BC molecules (24). Recently, chiral domains have been observed in a compound which exhibits the  $SmA_dP_A$  phase (25), which can signify the ferriphase described above.

One of the most original characteristic features of the liquid crystal layers in compounds with BC molecules is the spontaneous breaking of chiral symmetry as the molecules are tilted about the arrow axes (Figure 2). This removes all of the mirror planes of the layers, although the molecules themselves are achiral (26). As the breaking of the symmetry is spontaneous, both signs of chirality occur with equal probability. Thus, polarity leads to chirality in these layers with tilted BC molecules, although there are several examples in which the molecules are upright, in which the polarity does not lead to layer chirality. On the other hand, as Meyer realised in 1975 (see (27)), in compounds with rod-like molecules, molecular chirality is necessary for the smectic C (SmC) phase with tilted molecules to acquire layer polarisation. The mutual orientations between the tilt

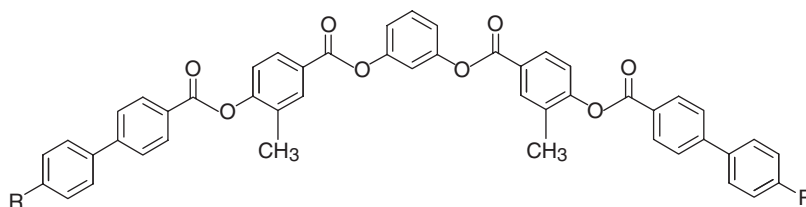


Figure 1. Structural formula of the bent core molecule 1,3 phenylene bis [4-(3-methylbenzoyloxy)] 4'-n-alkylbiphenyl 4'-carboxylate.

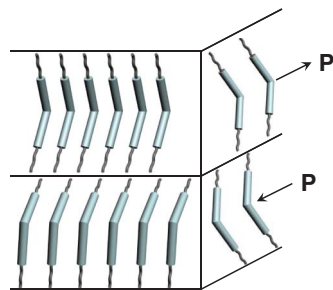


Figure 2. Schematic diagram showing the arrangement of tilted BC molecules in a pair of adjacent layers in the  $B_2$  phase. Each layer has no mirror plane and is thus chiral.

and polarisation vectors of adjacent layers of BC molecules can have four different combinations (26), all of which have been found, and are indicated by the common symbol  $B_2$ .

In general, the arrow axis need not be confined to the plane of the layer, but can tilt away from the plane. This is the most general possible tilt of the polar axis of the molecule. de Gennes had foreseen this possibility and named it smectic  $C_G$  ( $SmC_G$ ), where  $G$  stands for 'general'. As noted earlier, in liquid crystals made of BC molecules, tilt and polarisation are independent order parameters, and there is no linear coupling term between the two in the Landau free-energy density, unlike in ferroelectric liquid crystals made of rod-like molecules. An analysis of the relevant free energy (28, 29) shows that, apart from the tilted  $B_2$  and non-tilted structures mentioned earlier,  $SmC_G$  phases with both longitudinal ferroelectric and antiferroelectric order can be expected in suitable compounds. Some examples of the  $SmC_G$  phase have been reported (30).

The above liquid crystals with a layered arrangement in which the BC molecules are usually tilted are found in compounds with relatively long end chains, as in the case of the  $SmA$  and  $SmC$  phases exhibited by rod-like molecules. A large number of homologous series of compounds with BC molecules have been synthesised during the last decade. The most often observed sequence of liquid crystalline phases in a homologous series of compounds made of BC molecules is different from that in either rod-like or disc-like molecules. Usually the nematic phase is not found, except in some compounds in which the molecules have a relatively large opening angle between the two arms of the BC (21). Many of these nematogens also exhibit the calamitic  $SmA$  and  $SmC$  phases in which the layers do not have polar order (21). In the more typical compounds made of BC molecules with an opening angle of around  $120^\circ$ , the sequence of the phases is  $B_6$ – $B_1$ – $B_2$  (Figure 3). The  $B_6$  phase exhibited by the lower homologues also has a layered structure, but with intercalated molecules. The tilt angle is

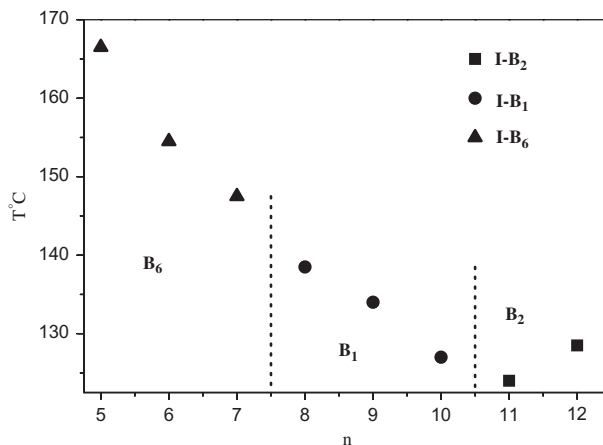


Figure 3. The phase diagram of the homologous series of compounds whose molecules have the general structural formula shown in Figure 1. The number of carbon atoms in each end chain is indicated by  $n$ . The figure is drawn using data from (62).

usually small or even zero. In the latter case the layer spacing corresponds to half the length of the BC molecule along the bow axis. The packing of the BC molecules in successive layers is antiferroelectric (Figure 4). There is a considerable overlap of the aromatic cores of molecules in one layer with the aliphatic chains of the molecules of neighbouring layers. As the chain length is increased further, in a few homologues with intermediate chain lengths, the  $B_1$  phase is observed. This has a two-dimensionally periodic structure, as in the columnar liquid crystal phases found in compounds with disc-like molecules. Each column is a ribbon in whose cross section a few BC molecules are packed in a strip with polar order.

The orientation of the polarisation vector was originally thought to be orthogonal to the column axis (Figure 4). More recent investigations appear to show

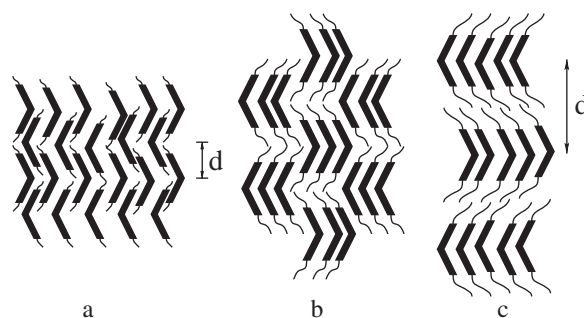


Figure 4. Schematic diagram showing the molecular arrangements in (a)  $B_6$ , (b)  $B_1$  and (c)  $SmAP_A$  liquid crystals. The layer spacings in the lamellar structures are indicated by  $d$ . Reproduced with permission from (34); copyright © 2005 European Physical Journal.

that in most cases, the polarisation is oriented along the column axis, with an antiferroelectric arrangement of neighbouring columns. Further, the polarisation has a splay distortion (31). The latter structure is sometimes described as the  $B_{1\text{rev}}$  phase. As mentioned earlier, as the chain length is increased further, the  $B_2$  phase with monomolecular layers with tilted molecules is found. Some compounds with special chemical groups exhibit variants such as the  $B_7$  phase, which has an exotic structure (32).

The  $B_2$  phase has a monolayer structure arising from a nano-segregation between the aromatic moieties and the long aliphatic chains, as in the case of the smectic phases made of rod-like molecules. The tilt of the molecules mainly arises because of the permanent dipoles attached to the aromatic cores. Assuming a symmetric structure of the two arms of the BC molecule, a dipole along the arrow axis results in a repulsive interaction between two neighbouring molecules which lie side by side (Figure 5). On the other hand, the interaction is attractive for molecules lying one behind the other. The repulsive interaction of the sideways-lying molecules can be reduced by a tilt about the arrow axes, as in the case of SmC liquid crystals (33). When the chains are short, the entropy of mixing of the chains and cores lowers the free energy more efficiently than the enthalpy gain from a nano-segregation between the two types of moieties. The bent shape of the molecules in turn favours the intercalated structure of the  $B_6$  phase, which ensures a better packing. For intermediate chain lengths, there is competition between the two types of layer structures. The result is the two-dimensionally modulated structure of the  $B_1$  phase, in which the overlap between the cores and

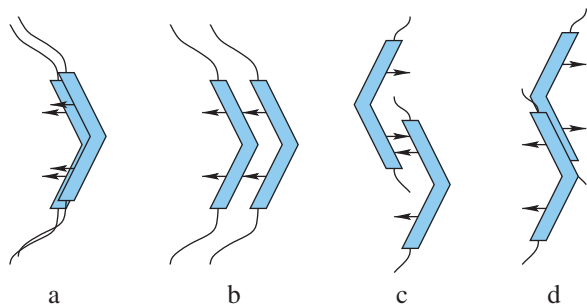


Figure 5. Schematic diagram showing the dipolar interactions in layers made of BC molecules. In a monolayer structure the dipoles have (a) an unfavourable sideways interaction leading to a tilting of the BC molecules about the arrow axes, and (b) a favourable interaction for a lining up of the molecules one behind the other in a polar cluster. In the intercalated layers (c) and (d), the dipolar interactions are usually favourable. Reproduced with permission from (34); copyright © 2005 European Physical Journal.

chains of neighbouring molecules is confined to the peripheral molecules of the ribbons. The physical origin of the  $B_1$  phase is thus reminiscent of that of the  $\text{Sm}\tilde{\text{A}}$  phase in some compounds made of rod-like molecules with strongly polar end groups (2).

The additional feature in the case of the BC molecules is the polar packings within layers of both types. A full description of the phase sequence requires several order parameters corresponding to the following: (a) the orientational order, which has a biaxial character and thus requires two parameters; (b) two translational order parameters corresponding to the two layer spacings mentioned above; (c) the polar order in each layer due to the packing constraint; and (d) the tilt order. As all of these order parameters are coupled, the resulting Landau free energy will have far too many terms, and the analysis becomes quite unwieldy. In order to keep the description simple and to bring out the basic mechanism giving rise to the observed sequence, the following assumptions have been made (34): (a) the tilt is ignored, as it is not essential for the packing model; (b) the medium is assumed to have perfect orientational order. The second assumption means that the highest temperature phase is nematic rather than the isotropic phase seen in most compounds. The frustrated packing model now has only three order parameters, and becomes tractable. The resulting phase diagram is shown in Figure 6 in the reduced temperature–reduced chain length plane (34). The structures of the three banana liquid crystals are as shown in Figure 4, the  $\text{SmAP}_A$  phase being the non-tilted version of the  $B_2$  phase with an antiferroelectric order of neighbouring layers. Note the overall similarity with the experimental phase diagram (Figure 3). As mentioned earlier, recent studies have shown that many compounds exhibit a variant of

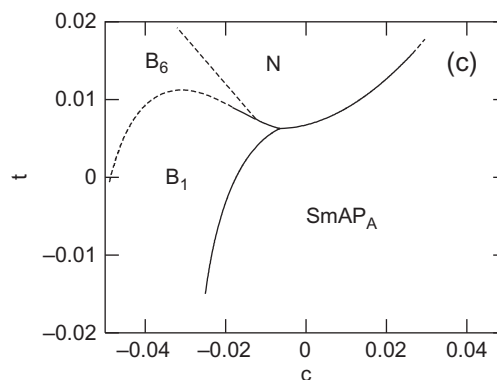


Figure 6. Theoretical phase diagram showing various phase transitions involving  $B_6$ ,  $B_1$ ,  $\text{SmAP}_A$  and nematic phases in the reduced temperature–reduced chain length plane. Reproduced with permission from (34); copyright © 2005 European Physical Journal.

the  $B_1$  phase in which the polar order is along the columnar axis rather than perpendicular to that as in Figure 4. This mutual orientation of the polar vectors with respect to the column axis means that the term ( $\delta$  in (34, Equation (4))) coupling the polar order and the transverse gradient of the order parameter characterising the  $SmAP_A$  structure takes a negative sign. In most series, a given homologue exhibits only one type of the banana liquid crystal (Figure 3). Some examples are now known that exhibit  $B_1$ – $B_6$  as well as  $B_1$ – $B_2$  transitions, in the temperature sequence predicted by the model (35).

Thus, the two-dimensionally periodic structures exhibited by the  $B_1$  phase or its variants can be thought of as arising from the competition between two different mechanisms generating two different types of layering order with polar packings: (i) the nanophase segregation between the aromatic cores and aliphatic chains, favoured for enthalpic reasons in higher members of the series, and (ii) the entropically favoured mixing of cores and chains which prevails in lower homologues. In the  $B_1$  phase the energetically unfavourable overlap between the cores and chains occurs only at the edges of the ribbons. Can we generate the  $B_1$  structure by manipulating the interactions near the edges? The answer is in the affirmative, as the following experimental results demonstrate.

### 3. Induced banana phases in mixtures of compounds with BC and rod-like molecules

Studies on binary mixtures are helpful in identifying the liquid crystal phases exhibited by newly synthesised compounds (2). If the two compounds of the mixture exhibit different types of liquid crystals, starting from one of the pure components, the transition point to the higher temperature phase is depressed as the concentration of the other component is increased, and a miscibility gap results (36). However, in some cases, specific interactions between the two types of molecules can lead to the induction of a new type of liquid crystal, which is not found in either component. A well-known example is the induction of SmA phase in mixtures of compounds whose molecules have the highly polar cyano or nitro end groups with those without such groups. Charge transfer complex formation between the two types of molecules leads to the induced SmA phase in such mixtures (37). Another type of binary mixture, which has attracted a large number of theoretical studies, is made of nematogens with rod-like and disc-like molecules. In this case, purely for geometric (and, hence, entropic) reasons the directors of the two types of molecule can be expected to be orthogonal to each other in the mixtures, thus leading to a biaxial nematic ( $N_b$ ) phase (38).

Experimental studies however show a phase separation between rod-rich and disc-rich nematic phases (39), as was indeed predicted by a detailed molecular model (40). Recent simulations indicate that a fine-tuning of the attractive interactions between the two types of molecules can give rise to the induced  $N_b$  phase (41).

BC molecules have the shape of bent rods, and nematogens made of BC and rod-like molecules can be expected to mix without any phase separation. The novel banana liquid crystals arise because of polar packings in layers or ribbons, as described above. If the compound with rod-like molecules exhibits the smectic C phase with synclinal tilt of neighbouring layers, addition of an appropriate compound with BC molecules even at a small concentration results in an anticlinic structure, which indicates that the BC molecules span a pair of neighbouring layers, reorienting the rods to be parallel to the arms of the BC molecules in the two layers (42).

After trying out several binary mixtures of the two types of compounds, we found interesting phase diagrams in some cases. We describe briefly the results on two systems (I and II). In both systems, the compound with BC molecules is the 12th homologue of the series whose phase diagram is shown in Figure 3. The compound denoted by the symbol BC12 exhibits the  $B_2$  phase, which as we described earlier, has a layered structure with tilted molecules. The structural formula of the compound 4-biphenyl 4'-n-undecyloxybenzoate (BO11) with rod-like molecules is shown in Figure 7. The alkyl chain is attached to only one end of this molecule. The compound exhibits bilayer SmA ( $SmA_2$ ) phase because of the nanosegregation between the aromatic and the aliphatic moieties, with a layer spacing equal to twice the molecular length. It also exhibits the nematic phase at higher temperatures. Thus, both components of the mixture have lamellar phases. The phase diagram of the mixture (Figure 8) shows that several liquid crystalline phases are induced, depending on the composition (43). The addition of BO11 leads to a sharp reduction of the  $B_2$ –Iso transition temperature, but interestingly, as the concentration exceeds 15 mol % of BO11, the  $B_1$  phase is induced. The two-dimensionally periodic structure is stable all the way up to approximately 63 mol % of BO11. Beyond this composition the  $B_6$  phase is induced,

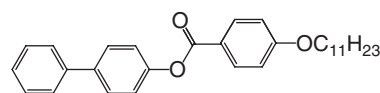


Figure 7. Structural formula of 4-biphenyl 4'-n-undecyloxybenzoate (BO11), used in the binary mixture system I.

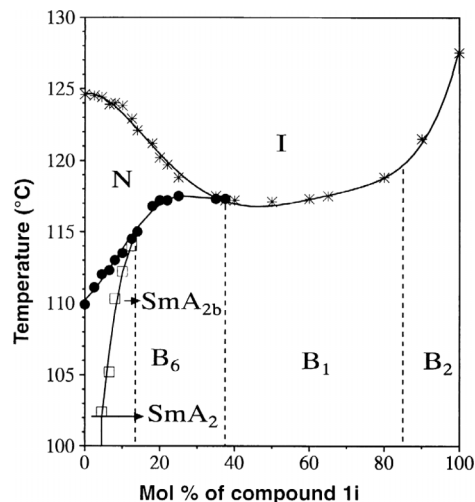


Figure 8. Phase diagram of the mixtures made of BC12 (indicated by 1i) and BO11 (system I). Reproduced with permission from (43); copyright © 2000 AAAS.

which is stable up to 87 mol% of BO11. Thus, increasing the concentration of the rod-like molecules has the same effect as decreasing the chain lengths of the BC molecules (Figure 3). In the highly rod-rich compositions above 87 mol % of BO11, another new type of calamitic phase is induced, which we describe later.

What is the origin of the stability of the induced phases? When the concentration of BO11 molecules is low, the rods are just distributed in the monolayers of the  $B_2$  phase. As the concentration of the rods is increased, they can lead to a break up of the layers into ribbons, which form the two-dimensionally periodic  $B_1$  phase, the rods acting like glue between adjacent ribbons (Figure 9). As the concentration of BO11 is increased further, the  $B_1$  phase is sustained all of the way up to approximately 63%, beyond which there are too many rods in the mixture, and the entropy of mixing of the two types of molecules favours the formation of the  $B_6$  phase (Figure 10). We may recall that the long dodecyl chains at the two ends of the BC molecules do not allow the latter to pack themselves in the intercalated layer structure of this phase, as the overlap between the aromatic and aliphatic moieties of molecules from neighbouring layers is highly unfavourable energetically. The BO11 molecules can position themselves between the BC molecules such that there is a partial overlap between the aromatic parts of the two types of molecules, thus reducing the unfavourable intermolecular energy mentioned earlier. The presence of an alkyl chain only at one end of the aromatic core of the BO11 molecule facilitates the formation of the intercalated structure of the  $B_6$  phase when the concentration of BO11 molecules is relatively high.

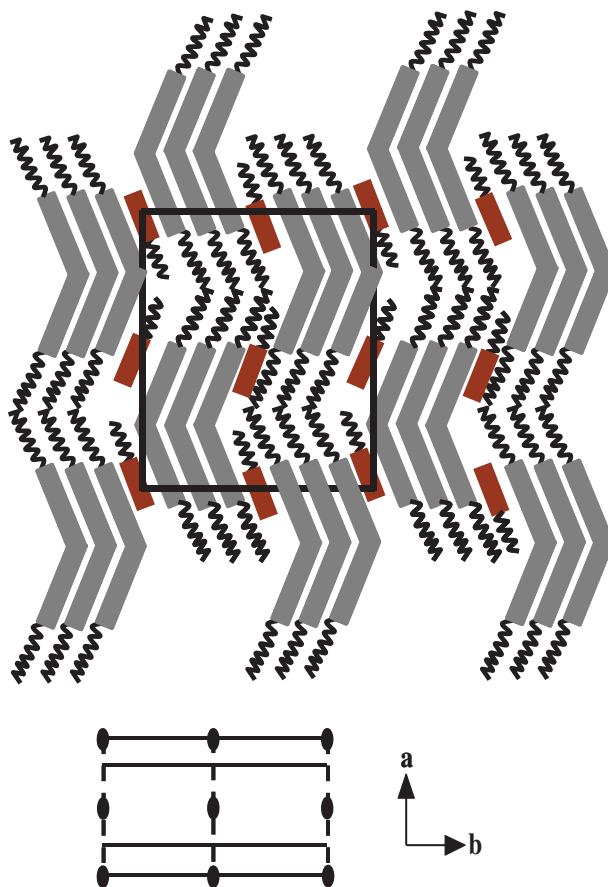


Figure 9. Schematic diagram showing the arrangement of molecules in the induced  $B_1$  phase in some mixtures of BC12 and BO11. The symmetry operations relevant to the structure are also indicated. Reproduced with permission from (45); copyright © 2005 the American Physical Society.

#### 4. Induced biaxial SmA phase at low concentrations of BC molecules

As the concentration of BO11 molecules is increased above 87 mol %, there are too few BC molecules to sustain the intercalated layer structure of the  $B_6$  phase. The layer structure now changes over to that of the smectic  $A_2$  phase characteristic of the BO11 molecules. How will the BC molecules arrange themselves in the layers? The nanosegregation of the aromatic and aliphatic moieties leads to the formation of the bilayer smectic phase of BO11. The BC molecules have aromatic bent cores and long alkyl chains, and can be expected to be accommodated in the bilayers. Indeed starting from pure BO11, the  $SmA_2$ -N transition point increases as the concentration of the BC molecules is increased (Figure 8). More interestingly, when the concentration of the BC molecules exceeds approximately 4.5 mol %, the  $SmA_2$  undergoes a transition to a new induced phase as the temperature is lowered. Using various physical studies, the latter was shown to be a

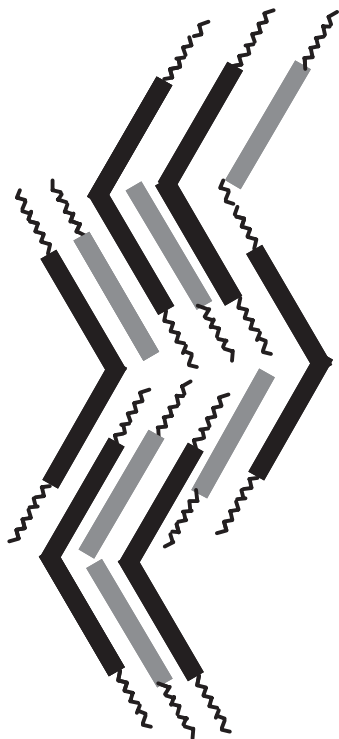


Figure 10. Schematic diagram showing the arrangement of molecules in the induced B<sub>6</sub> phase in some mixtures of BC12 and BO11.

biaxial SmA<sub>2</sub> (SmA<sub>2b</sub>) phase. The SmA<sub>2</sub>–SmA<sub>2b</sub> transition point rapidly increases with the concentration of BC molecules. The BC molecules undergo an orientational transition across the phase transition point (43). As described earlier, above about 13 mol% of BC molecules, the B<sub>6</sub> phase dominated by the packing constraints of the BC molecules replaces the SmA<sub>2</sub> phase. Our physical studies pointed to an organisation of the BC molecules with their bow axes lying in the smectic layer planes (Figure 11) in the SmA<sub>2</sub> and SmA<sub>2b</sub>

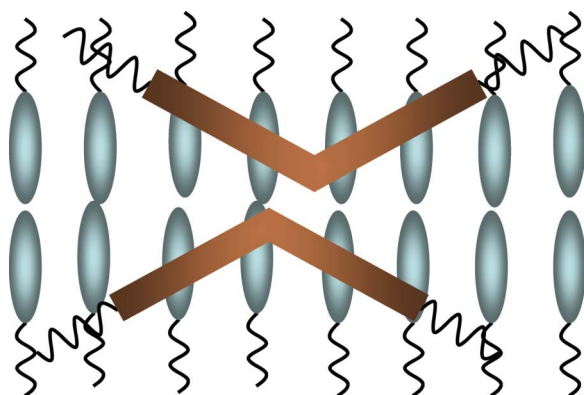


Figure 11. Schematic diagram showing the arrangement of molecules in the induced biaxial SmA phase in some mixtures of BC12 and BO11.

phases. This structure also leads to a nanosegregation between the aromatic cores and aliphatic chains of the BC molecules in the appropriate parts of the SmA<sub>2</sub> layers made of BO11 molecules. Indeed the enthalpic gain due to the nanosegregation appears to be essential for the stability of the proposed structure. Computer simulations on mixtures of hard BC molecules with hard rods do not support the occurrence of the above structure (44). The hard rods by themselves exhibit the SmA phase, and even approximately 3% of BC molecules with the same length to diameter ratio as the rods induces the anticlinic SmC<sub>A</sub> phase in which the rods are tilted in opposite directions in neighbouring layers. Experimentally, a ferroelectric SmC\* liquid crystal made of rod-like molecules has been shown to exhibit an antiferroelectric phase on doping with a compound with BC molecules (42).

In order to investigate further the influence of the nanosegregation on the molecular arrangements in mixtures of rod-like and BC molecules, we investigated a second system consisting of mixtures of the BC12 compound with 4-n-octyloxy 4'-cyanobiphenyl (8OCB, Figure 12), a well-studied compound with highly polar rod-like molecules (45).

8OCB exhibits nematic and partially bilayer SmA<sub>d</sub> phases, the layer spacing in the smectic phase being about 1.4 times larger than the molecular length. The latter is a consequence of the antiparallel orientation of near-neighbour molecules, which is favoured by the electrostatic interactions between the polar groups, and an overlap of the aromatic moieties, which results from the nanosegregation described earlier. The phase diagram is somewhat different from the first system. The B<sub>1</sub> phase is induced between 35 and 60 mol % of the BC molecules. The 8OCB pairs appear to remain intact in the mixtures, and act as the glue between the ribbons of BC molecules (45). However, as the pairs have chains at both ends, the intercalated B<sub>6</sub> phase is not found at higher concentrations of 8OCB molecules. Instead, the 8OCB molecules form the partial bilayers, and the BC molecules are confined with their arrow axes normal to the layers, as in the biaxial smectic phase of the system I. However, for concentrations lying between approximately 24 and 35 mol % of BC molecules, the latter organise themselves in a periodic arrangement within the smectic layers as shown in Figure 13. The resulting two-dimensionally periodic structure has *c2mm* symmetry. We denote this

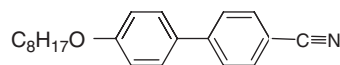


Figure 12. Structural formula of 4-n-octyloxy 4'-cyanobiphenyl (8OCB), used in the binary mixture system II.



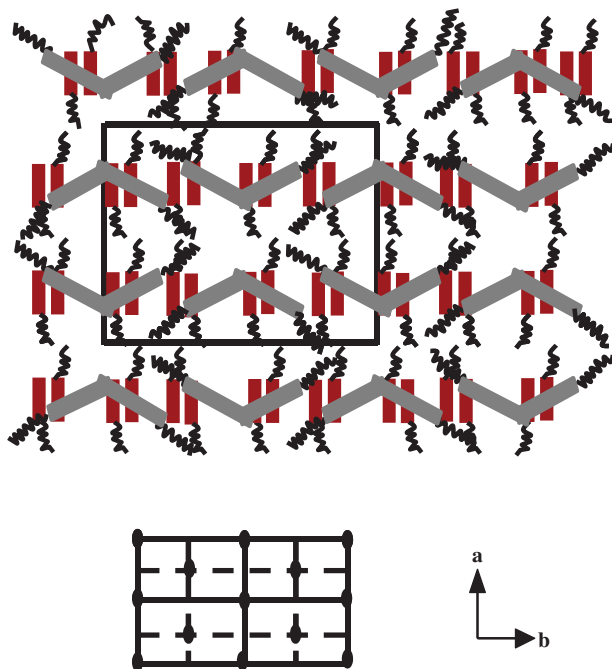


Figure 13. Schematic diagram showing the arrangement of molecules in the induced  $B_1'$  phase in some mixtures of BC12 and 8OCB. The symmetry operations relevant to the structure are also indicated. Reproduced with permission from (45); copyright © 2005 the American Physical Society.

phase by the symbol  $B_1'$ , to distinguish it from the  $B_1$  phase stabilised between 35 and 60 mol % of BC molecules. For concentrations lying below approximately 24 mol % of BC molecules, the periodicity of BC molecules within the layers is lost and the biaxial  $SmA_{db}$  phase is obtained. For concentrations below about 15 mol % of BC molecules, the  $SmA_{db}$  goes over to the uniaxial  $SmA_d$  phase as the temperature is increased. As in the system I, the  $SmA_{db}$ – $SmA_d$  or  $SmA_{db}$ –N transition temperature increases rapidly with the concentration of the BC molecules, which simply reflects the fact that the relevant low-temperature phase owes its origin entirely to the BC molecules. However, unlike in the system I, the  $SmA_d$ –N transition temperature decreases, while the N–I transition point increases as the concentration of the BC molecules is increased, starting from zero (45). This clearly indicates that the BC molecules do not fit snugly in the partial bilayers of 8OCB molecules. The spacing corresponding to the 8OCB layers of the  $B_1'$  phase is approximately 28 Å, which is somewhat smaller than that in pure 8OCB. The BC molecules have ester linkage groups while the 8OCB molecules have cyano groups. This has been exploited to confirm the proposed mutual alignment (Figure 11) of the two types of molecules in the smectic phases (45) by conducting polarised infrared spectroscopic measurements on an aligned sample of the mixture.

Another binary system, made of mixtures of rod-like and BC molecules, has been studied by Zhu *et al.* (46). The system consists of rod-like chiral molecules indicated by the symbol TFMHPOBC with an enantiomeric excess of 0.2, and exhibits a higher-temperature phase with synclinal layers with tilted molecules, which goes over to a phase in which neighbouring layers have anticlinal tilt, as the temperature is lowered. Studies on various mixtures of this compound with 1,3-phenylene bis[4-(4-heptylphenyliminomethyl)benzoate], a compound made of BC molecules, show that the latter tend to suppress the phase with synclinal layers. At very low concentrations, the BC molecules are arranged with their two arms lying in two neighbouring layers such that their arrow axes are also parallel to the layer plane, and the bow axes are oriented along the layer normal. Curiously, for compositions with more than 3 wt% of the BC molecules, a reorientation of the BC molecules takes place as the temperature is lowered to a specific transition point. Below this temperature, the BC molecules lie in only one monolayer, with their arrow axes tilted appropriately, and now the bow axes lie in the layer plane (46). This mutual orientation of the two types of molecules is reminiscent of that in the  $SmA_b$  phase described above.

Returning to the mixtures of 8OCB and BC12, the schlieren texture of the biaxial smectic phase is seen in cells made of uncoated glass plates, or in free-standing films (47). Further, the focal conic domains in the  $SmA_{db}$  phase are found to be associated with topologically non-trivial configurations of the banana director field ( $n_b$ ) in the surrounding matrix. The composition is essentially uniform in these samples. We recently found that a strikingly new texture is obtained if the sample is taken between unidirectionally rubbed glass plates (48). The sample now exhibits a stripe pattern, in which alternate domains are in the uniaxial  $SmA_d$  and biaxial  $SmA_{db}$  phases. Between appropriately placed crossed polarisers, the sample exhibits alternate dark and bright bands corresponding to the domains in the two phases (Figure 14). The banana director  $n_b$  orients along the rubbing direction, while the director corresponding to the long axes of the 8OCB molecules  $n_r$  orients normal to the glass plates. In most samples, the stripes are straight, and the corresponding wave vector  $q_s$  makes an angle  $\omega_0$  of about 30° to 50° with  $n_b$ . Other fluids exhibiting stripes are Langmuir monolayers, and ferrofluids subjected to an external magnetic field. In these systems, the stripe patterns arise from competition between short-range attractive and long-range dipolar interactions which are repulsive in nature (49). A notable difference between these systems and the liquid crystals is in the nature of the defects: edge dislocations occur in the former, while lattice disclinations are found in the latter (48).



Figure 14. Photograph of the stripe texture exhibited by a mixture of BC12 and 8OCB, taken between rubbed glass plates. Reproduced with permission from (48); copyright © 2007 Europhysics Letters.

The stripes in the liquid crystal system are only seen between rubbed glass plates. The rubbing action generates a positive charge density  $\sigma$  on the glass plates. The liquid crystal usually has ionic impurities, and the ion distribution should obey the Poisson–Boltzmann distribution, modified by the periodic potential due to the smectic layering (50). Theoretical studies have shown that a periodic modulation of the surface charge density  $\sigma$  lowers the electrostatic energy of an electrolytic cell (51). The stripe formation appears to be a visual manifestation of this underlying periodic charge distribution (48).

### 5. Physical properties of nematic liquid crystals made of mixtures of rod-like and BC molecules

The rod-rich compositions of system II also exhibit the uniaxial nematic phase over fairly wide ranges of temperature. This allows for studies on the influence of the BC molecules on various physical properties in the nematic phase. The optical birefringence decreases with the concentration of the BC molecules ( $x_{BC}$ ), as the latter have a lower anisotropy of polarisability than the rod-like molecules (52). The dielectric anisotropy decreases rapidly with  $x_{BC}$ . As the net dipole moment is orthogonal to the bow axis of the BC molecule, the rapid fall implies that the bow axes of the BC molecules align along the nematic director defined by the long axes of the 8OCB molecules, unlike in the SmA phases.

The former mutual orientation in the nematic is favoured entropically. The splay elastic constant also decreases as  $x_{BC}$  is increased (Figure 15(a)), mainly because the BC molecules have a bent structure, and do not pack well in the nematic phase. In the mixture with 17 mol % of BC molecules,  $K_{11}$  decreases by about 35% compared with that in pure 8OCB. The more interesting result is that unlike in pure 8OCB, in all of the mixtures studied, the splay constant falls sharply as the N–SmA<sub>d</sub> transition point is approached. This

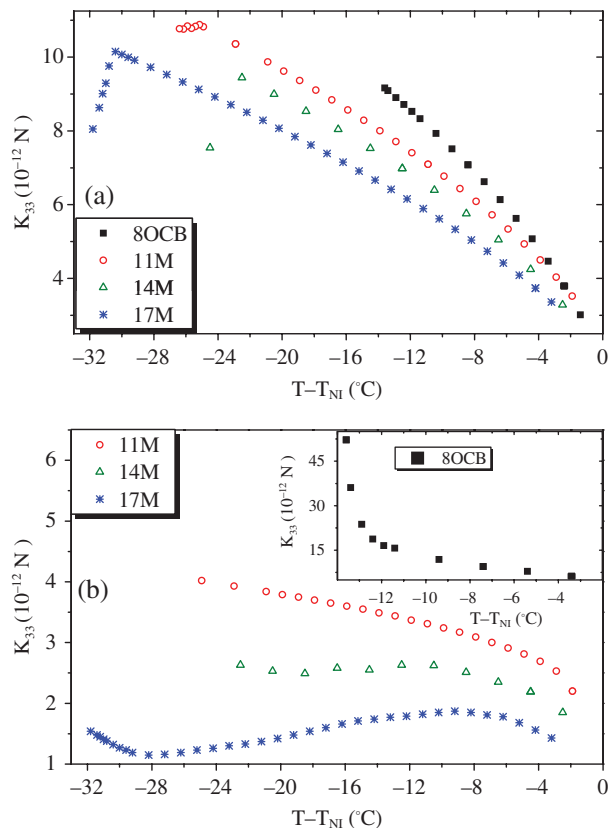


Figure 15. Dependences of (a) splay and (b) bend elastic constants of pure 8OCB and three mixtures of 8OCB and BC12 on the relative temperatures. The symbol  $xM$  stands for  $x$  mol % of BC molecules. Reproduced with permission from (52); copyright © 2007 the American Physical Society.

clearly shows that the BC molecules align with their arrow axes along the layer normal of the smectic-like short-range ordered groups which build up as the transition point is approached. The bent shape of the BC molecule now facilitates a splay distortion of the director field of the rod-rich nematic (Figure 16(b)). This in turn leads to the sharp fall in  $K_{11}$ . The more dramatic effect of the BC molecules is naturally found in the bend elastic constant. Dodge *et al.* (53) had earlier found that  $K_{33}$  can reduce by a factor of two by adding just approximately 3 mol % of BC molecules to a nematic made of rod-like molecules. In the mixtures studied by us, we can have much higher concentrations of the BC molecules. The results are shown in Figure 15(b). The bend constant decreases by a factor of four in the mixture with 11 mol % of BC molecules. As the concentration of BC molecules is increased further, interestingly  $K_{33}$  increases initially as the temperature is lowered from the N–I transition point, attains a maximum value, and shows an anomalous decrease as the temperature is lowered further. It increases again only close to the N–SmA<sub>d</sub> transition point, owing to the

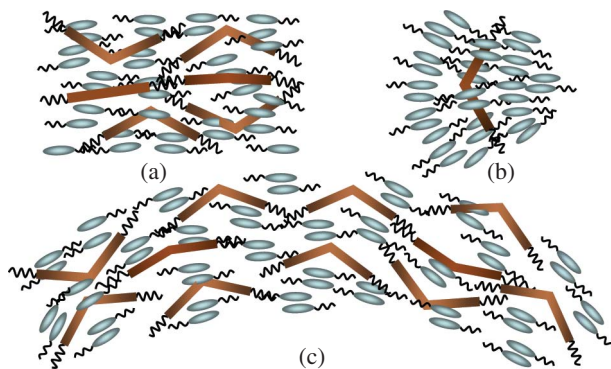


Figure 16. (a) Mutual alignment of 8OCB dimers and BC12 molecules in the nematic phase. (b) When the smectic-like short-range order builds up, the BC molecules reorient and facilitate a splay distortion of the director. (c) In the nematic phase, the BC molecules facilitate a bend distortion of the director. Reproduced with permission from (52); copyright © 2007 the American Physical Society.

build up of smectic-like short-range order. The drastic lowering of  $K_{33}$  and its anomalous temperature dependence confirm that the BC molecules are oriented with their bow axes along the nematic director (Figure 16(a)), except close to the N–SmA<sub>d</sub> transition point. The bent shape of the BC molecule facilitates a bend distortion of the director field (Figure 16(c)), lowering  $K_{33}$ . Indeed the molecular shape couples better to the director distortion if the orientational order is better developed. In the mean field approximation, we can write  $K_{ii} = K_{i0}S^2$ . Adding the BC molecules reduces both the splay and bend constants and we can write  $K_{i0} = (K_i^r - \alpha_i x_{BC})$  where  $K_i^r$  corresponds to pure 8OCB. In the case of the bend distortion, as we argued above, the coupling between the molecular shape and the director distortion becomes stronger with the order parameter, and we can write  $\alpha_3 = \beta_3 S$ . This immediately shows that  $K_{33}$  exhibits a maximum as a function of the order parameter, at the value  $S_m = 2K_3^r / (3\beta_3 x_{BC})$ . As the concentration  $x_{BC}$  is increased, the maximum of  $K_{33}$  occurs at a lower value of the order parameter, i.e. at a higher temperature (52).

In the usual nematics made of rod-like molecules such as 8OCB, the bend constant is larger than the splay constant. On the other hand, in the mixtures with BC molecules, the elastic anisotropy has a reversed sign, and has a large magnitude for the mixture with 17 mol% of BC molecules. This causes the electro-optic response in the mixtures to have a much sharper variation with voltage above the threshold than in the nematics made of rods only (Figure 17). The sharp response may be useful in device applications. Mixtures in which the concentration of BC molecules is increased to approximately 20 mol % exhibit another interesting feature. Using a homeotropically aligned

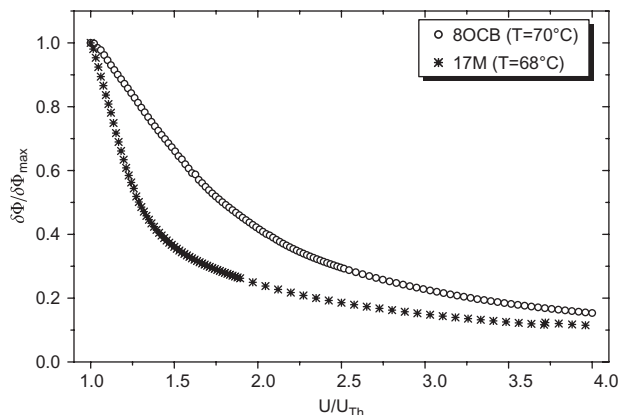


Figure 17. The voltage dependences of the normalised optical phase difference  $\delta\Phi/\delta\Phi_{max}$  for pure 8OCB and for the mixture 17M, above the threshold voltage.

sample with a thickness of approximately  $9\ \mu\text{m}$  to measure  $\epsilon_{||}$  directly, the latter is found to increase by about 2% in the nematic phase if the measuring voltage is increased from 10 to 30 V (54). In the case of pure 8OCB, the increase is far smaller, less than 0.2% for a similar applied field (55). In 8OCB, the enhancement of  $\epsilon_{||}$  reflects that of the order parameter, and mainly arises from a quenching of the director fluctuations, as was pointed out by de Gennes (2). In the mean field model the enhancement in the order parameter is proportional to  $(\Delta\epsilon/K^3)^{1/2}$ , where  $K$  is an average elastic constant. The mixture has an extremely low value of the bend elastic constant  $K_{33}$ . The elastic anisotropy can be taken into account to derive a formula for the quenching of the director fluctuations by an electric field applied parallel to the director. The calculated enhancement in  $S$  is approximately 0.5%, which is still considerably smaller than the experimental value. The molecular weights of BC12 and 8OCB are 1142 and 307 respectively, which means that at 20 mol%, the BC molecules occupy more than half the volume. The minimum energy conformation of BC12 shows that the molecule has a dipole moment of approximately 4 Debye oriented along the arrow axis. The electrostatic interaction between the BC molecules as well as their compact packing favour a clustering with two or more molecules lining up one behind the other (see Figure 5). These clusters have a proportionately higher net dipole moment depending on the size, compared with that of a single BC12 molecule. This is in contrast to the dipolar effect in the rod-like 8OCB molecules, which leads to the formation of antiparallel pairs as noted earlier (13). The polar axis of the cluster can in turn reorient under a large electric field to enhance  $\epsilon_{||}$ .

Flexoelectricity is another property of the nematic, which can be strongly influenced by the bent shape of the BC molecules. Meyer originally proposed that

flexoelectric properties arise in nematics made of pear-shaped molecules with longitudinal dipoles or banana-shaped molecules with transverse dipoles (56). It became clear later (57) that due to the contribution from the quadrupolar densities resulting from the quadrupolar order, flexoelectricity is a universal property of all nematics. Nevertheless, as the BC12 molecules have the characteristics envisaged by Meyer, they can be expected to make a strong dipolar contribution to flexoelectricity. Molecular models (58) predict that the dipolar contribution to  $e_{33}$ , the flexoelectric coefficient associated with the bend distortion of the director field, is proportional to the kink angle  $\Theta$ , which is zero for a rod and approximately  $60^\circ$  in BC12. We can expect that BC12 can contribute significantly to the  $e_{33}$  value of the mixtures. The action of a transverse DC electric field on the flexoelectric polarisation of the distorted director field in a hybrid aligned nematic (HAN) cell can be used to measure  $(e_{11} - e_{33})$ , which arises entirely from the dipolar effect (59). Measurements show that  $(e_{11} - e_{33})/K$ , where  $K$  is an average elastic constant, doubles in magnitude by adding just 5 mol % of BC12 molecules to 8OCB. Assuming a simple additivity rule, the result implies that  $(e_{11} - e_{33})/K$  of BC12 is about 20 times larger than that of 8OCB (54). Interestingly, a mixture with approximately 10 mol % of BC12 yielded only a homeotropically aligned director, even though one of the plates of the HAN cell was coated with SiO at a grazing angle of approximately  $30^\circ$  which would favour a planar alignment. The flexoelectric polarisation  $\mathbf{P}$  generates an electric field, and if the field is not screened out by dissolved ionic charges, the self-energy due to  $\mathbf{P}$ , which depends quadratically on the product of a relevant flexocoefficient and curvature, effectively increases the elastic constants, as was noted by de Gennes (2). As the concentration of BC molecules is increased to 10 mol %, the flexoelectric coefficient  $e_{33}$  of the mixture becomes large enough for the cell to become uniformly aligned: the enhanced effective elastic energy of a distorted director overcomes the relatively weak anchoring of the SiO coated plate. Indeed a pure BC nematogen, namely, 4-chloro-1,3-phenylene bis 4-[4'-(9-decenyloxy) benzyloxy] benzoate (Cl-BB for short) showed only a planar alignment in a cell treated for HAN configuration (60). In this case,  $e_{33}$  which was measured using a mechanical technique, was found to be rather large, about 1000 times that of a typical calamitic nematogen. This huge value probably means that in the pure BC compound the BC molecules form fairly large polar clusters mentioned earlier. Curiously, the bend elastic constant  $K_{33}$  of this compound is found to be comparable to that in a calamitic nematogen (61), and not negligibly small

as might have been expected from our measurements on mixtures. Further, it is only slightly larger than  $K_{11}$ . The probable reason for this result is the effective enhancement of  $K_{33}$  due to the large value of  $e_{33}$ .

In conclusion, the lowered symmetry of BC molecules introduces many new aspects to the complexity of the liquid crystalline phases, compared with those formed by rod-like and disc-like molecules. While the latter two types of molecules do not mix in the liquid crystalline phases, rod-like molecules have been shown to mix with the BC molecules to induce new phases not found in either. Some properties of the uniaxial nematic phase are strongly influenced by the bent shape of the molecules. We have summarised only some aspects of the fascinating field, in which we have made contributions. It is clear that many ideas introduced by de Gennes for describing physical properties of liquid crystals made by rod-like molecules are applicable to the new systems as well.

#### Acknowledgements

The work reported in the article was carried out in collaboration with B. K. Sadashiva, R. Pratibha, Arun Roy and Brindaban Kundu.

#### References

- (1) de Gennes, P.G. *Rev. Mod. Phys.* **1992**, *64*, 645–648.
- (2) de Gennes, P.G.; Prost, J. *The Physics of Liquid Crystals*, 2nd edn; Clarendon Press: Oxford, 1993.
- (3) Chandrasekhar, S. *Liquid Crystals*, 2nd edn; Cambridge University Press: Cambridge, 1992.
- (4) Kitzerow, H.; Bahr, C. *Chirality in Liquid Crystals*; Springer: Berlin, 2001.
- (5) McMillan, W.L. *Phys. Rev. A* **1971**, *4*, 1238–1246.
- (6) Chandrasekhar, S.; Savithramma, K.L.; Madhusudana, N.V. In *Liquid Crystals and Ordered Fluids*, Griffin, A.C. and Johnson, J.F., Eds; Plenum Press: New York, 1984; Vol. IV; pp. 299–309.
- (7) Feldkamp, G.E.; Handschy, M.A.; Clark, N.A. *Phys. Lett. A* **1981**, *85*, 359–362.
- (8) Goodby, J.W.; Waugh, M.A.; Chin, E.; Pindak, R.; Patel, J.S. *Nature* **1989**, *337*, 449–452.
- (9) Isaert, N.; Navailles, L.; Barois, P.; Nguen, H.T. *J. Physique II* **1994**, *4*, 1501–1518.
- (10) Renn, S.R.; Lubensky, T.C. *Phys. Rev. A* **1988**, *38*, 2132–2147.
- (11) Pramod, P.A.; Pratibha, R.; Madhusudana, N.V. *Curr. Sci.* **1997**, *73*, 761–765.
- (12) Fernsler, J.; Hough, L.; Shao, R.; MacLennan, J.; Navailles, L.; Brunet, M.; Madhusudana, N.V.; Mondain-Monval, O.; Boyer, C.; Zasadzinski, J.; Rego, J.A.; Walba, D.M.; Clark, N.A. *Proc. Natl. Acad. Sci. U.S.A.* **2005**, *102*, 14191–14196.
- (13) Madhusudana, N.V.; Chandrasekhar, S. *Pramana (Suppl.)* **1975**, *1*, 57–68.
- (14) Leadbetter, A.J.; Richardson, R.; Colling, C.N. *J. Phys. Colloq.* **1975**, *36 C1*, 37–43.

- (15) de Gennes, P.G. *Solid State Commun.* **1972**, *10*, 753–756.
- (16) Vorlander, D.; Apel, A. *Ber. Dtsch. Chem. Ges.* **1932**, *65*, 1101–1109.
- (17) Pelzl, G.; Wirth, I.; Weissflog, W. *Liq. Cryst.* **2001**, *28*, 969–972.
- (18) Matsunaga, Y.; Miyamoto, S. *Mol. Cryst. Liq. Cryst.* **1993**, *237*, 311–317.
- (19) Niori, T.; Selkine, T.; Watanabe, J.; Furukawa, T.; Takezoe, H. *J. Mater. Chem.* **1996**, *6*, 1231–1233.
- (20) Roy, A.; Madhusudana, N.V. *Europhys. Lett.* **1997**, *39*, 335–339.
- (21) Takezoe, H.; Takanishi, Y. *Jpn. J. Appl. Phys.* **2006**, *45*, 597–625.
- (22) Roy, A.; Madhusudana, N.V. *Europhys. Lett.* **1996**, *36*, 221–226.
- (23) Cepic, M.; Zeks, B. *Mol. Cryst. Liq. Cryst.* **1995**, *263*, 61–67.
- (24) Nadasi, H.; Weissflog, W.; Eremin, A. Pelzl, G.; Diele, S.; Das, B.; Grande, A. *J. Mater. Chem.* **2002**, *12*, 1316–1324.
- (25) Takezoe, H. (Private communication), 2009.
- (26) Link, D.R.; Natale, G.; Shao, R.; MacLennan, J.E.; Clark, N.A.; Korblova, E.; Walba, D.M. *Science* **1997**, *278*, 1924–1927.
- (27) Meyer, R.B.; Liebert, L.; Strzelecki, L.; Keller, P. *J. Phys. Lett.* **1975**, *36*, 69–72.
- (28) Roy, A.; Madhusudana, N.V.; Tolédano, P.; Figueiredo Neto, A.M. *Phys. Rev. Lett.* **1999**, *82*, 1466–1469.
- (29) Brand, H.R.; Cladis, P.; Pleiner, H. *Eur. Phys. J. B.* **1998**, *6*, 347–353.
- (30) Jakli, A.; Krüerke, D.; Sawade, H.; Heppke, G. *Phys. Rev. Lett.* **2001**, *86*, 5715–5718.
- (31) Coleman, D.A.; Jones, C.D.; Nakata, M.; Clark, N.A.; Walba, D.M.; Weissflog, W.; Fodor-Csorba, K.; Watanabe, J.; Novotna, V.; Hamplova, V. *Phys. Rev. E* **2008**, *77*, 021703 (1–6).
- (32) Coleman, D.A.; Fernsler, J.; Chattham, N.; Nakata, M.; Takanishi, Y.; Korblova, E.; Link, D.R.; Shao, R.F.; Jang, W.G.; MacLennan, J.E.; Mondainn-Monval, O.; Boyer, C.; Weissflog, W.; Pelzl, G.; Chien, L.C.; Zasadzinski, J.; Watanabe, J.; Walba, D.M.; Takezoe, H.; Clark, N.A. *Science* **2003**, *301*, 1204–1211.
- (33) Govind, A.S.; Madhusudana, N.V. *Europhys. Lett.* **2001**, *55*, 505–511.
- (34) Roy, A.; Madhusudana, N. *Eur. Phys. J. E* **2005**, *18*, 253–258.
- (35) Folcia, C.L.; Etxebarria, J.; Ortega, J.; Ros, M.B. *Phys. Rev. E* **2006**, *74*, 031702 (1–6).
- (36) Doman, M.; Billard, J. *Pramana (Suppl.)* **1975**, *1*, 131–154.
- (37) Park, J.W.; Bak, C.S.; Labes, M.M. *J. Am. Chem. Soc.* **1975**, *97*, 4398–4400.
- (38) Alben, R. *J. Chem. Phys.* **1973**, *59*, 4299–4304.
- (39) Pratibha, R.; Madhusudana, N.V. *Mol. Cryst. Liq. Cryst. Lett.* **1985**, *1*, 111–116.
- (40) Palfy-Muhoray, P.; de Bruyn, J.; Dunmur, D.A. *Mol. Cryst. Liq. Cryst.* **1985**, *127*, 301–319.
- (41) Cuetos, A.; Galindo, A.; Jackson, G. *Phys. Rev. Lett.* **2008**, *101*, 237802 (1–4).
- (42) Gorecka, E.; Nakata, M.; Mieczkowski, J.; Takanishi, Y.; Ishikawa, K.; Watanabe, J.; Takezoe, H.; Eichhorn, S.H.; Swager, T.M. *Phys. Rev. Lett.* **2000**, *85*, 2526–2529.
- (43) Pratibha, R.; Madhusudana, N.V.; Sadashiva, B.K. *Science* **2000**, *288*, 2184–2187.
- (44) Maiti, P.K.; Lansac, Y.; Glaser, M.A.; Clark, N.A. *Phys. Rev. Lett.* **2002**, *88*, 065504 (1–4).
- (45) Pratibha, R.; Madhusudana, N.V.; Sadashiva, B.K. *Phys. Rev. E* **2005**, *71*, 011701 (1–12).
- (46) Zhu, M.H.; Dodge, M.R.; Shioda, T.; Rosenblatt, C.; Parker, D.D.; Kim, J.M.; Newbert, M.E. *Liq. Cryst.* **2004**, *31*, 1381–1386.
- (47) Smalyukh, I.I.; Pratibha, R.; Madhusudana, N.V.; Lavrentovich, O.D. *Eur. Phys. J. E* **2005**, *16*, 179–191.
- (48) Pratibha, R.; Madhusudana, N.V.; Sadashiva, B.K. *Europhys. Lett.* **2007**, *80*, 46001 (1–5).
- (49) Seul, M.; Andelman, D. *Science* **1995**, *267*, 476–483.
- (50) Roy, A.; Madhusudana, N.V. *Europhys. Lett.* **2008**, *84*, 36006 (1–6).
- (51) Lukatsky, D.B.; Safran, S.A. *Europhys. Lett.* **2002**, *60*, 629–635.
- (52) Kundu, B.; Pratibha, R.; Madhusudana, N.V. *Phys. Rev. Lett.* **2007**, *99*, 247802 (1–4).
- (53) Dodge, R.M.; Rosenblatt, C. Petschek, R.G.; Neubert, M.E.; Walsh, M.E. *Phys. Rev. E* **2000**, *62*, 5056–5063.
- (54) Kundu, B.; Roy, A.; Pratibha, R.; Madhusudana, N.V. (In preparation).
- (55) Basappa, G.; Madhusudana, N.V. *Mol. Cryst. Liq. Cryst.* **1996**, *288*, 161–174.
- (56) Meyer, R.B. *Phys. Rev. Lett.* **1969**, *22*, 918–921.
- (57) Prost, J.; Marcerou, J.P. *J. Physique* **1977**, *38*, 315–324.
- (58) Osipov, M.A. *Sov. Phys. JETP* **1983**, *58*, 1167–1171.
- (59) Dozov, I.; Martinot-Lagarde, P.; Durand, G. *J. Phys. Lett.* **1982**, *43*, L365–L369.
- (60) Harden, J.; Mbang, B.; Éber, N.; Fodor-Csorba, K.; Sprunt, S.; Gleeson, J.T.; Jakli, A. *Phys. Rev. Lett.* **2006**, *97*, 157802 (1–4).
- (61) Wiant, D.; Gleeson, J.T.; Éber, N.; Fodor-Csorba, K.; Jakli, A.; *Phys. Rev. E* **2005**, *72*, 041712 (1–4).
- (62) Sadashiva, B.K.; Raghunathan, V.A.; Pratibha, R. *Ferroelectrics* **2000**, *243*, 249–260.